Electronic Supplementary Information (ESI)

Improving the Performance of Supercapacitors by Combining Polymeric Redox Couples and a Polymer Hydrogel Separator

Xiaohong Liang,[a] Jiang Wu,[b] Zan Hua,*[b] and Guangming Liu*[a]

a. Department of Chemical Physics, Key Laboratory of Surface and Interface Chemistry and Energy Catalysis of Anhui Higher Education Institutes, Hefei National Research Center for Physical Sciences at the Microscale, University of Science and Technology of China, Hefei, 230026, P. R. China.
b. Biomass Molecular Engineering Center and Department of Materials Science and Engineering, Anhui Agricultural University, Hefei, 230036, P. R. China.

Materials and methods

Materials. Graphene (the Sixth Element (Changzhou) Materials Technology Co., Ltd.), propylsulfonate dimethylammonium propylmethacrylamide (PDP, 98%, Changzhou YiPinTang Chemical Co., Ltd.), 2,2,6,6-tetramethyl-4-piperidyl methacrylate (TMPM, 98.0%, TCI), 4,4'-azobis(4-cyanovaleric acid) (ACVA, 98.0%, Sigma-Aldrich), lithium chloride (LiCl, 99.0%, Aladdin), N-methyl-4,4'-bipyridinium iodide (MBI, 95%, Jiangsu Aikon Biopharmaceutical R&D Co., Ltd.), nafion 117 solution (N117, ~ 5 wt% in a mixture of lower aliphatic alcohols and water, Sigma-Aldrich), 4-hydroxy-2,2,6,6-tetramethypiperidine 1-oxyl free radical (4-OH-TEMPO, 98.0%, TCI), alpha-ketoglutaric acid potassium salt (98%, Sigma-Aldrich), acetonitrile (99%, Aladdin), 1,3-propanesulfonate (99%, Aladdin), and N-[3-(dimethylamino)propyl]acrylamide (DMAPAA, 97.0%, ~ 0.5% MEHQ as stabilizer, Aladdin) were all used as received. Hydrochloric acid (HCl, 36.0-38.0 wt%), hydrogen peroxide aqueous solution (H_2O_2, 30.0 wt%), and ethylenediamine tetraacetic acid (EDTA, 99.5%) were all purchased from Sinopharm Chemical Reagent Co., Ltd. and used as received. 4-Vinylbenzyl chloride (98%, Macklin) was used after purification with a basic alumina column.

Synthesis of the PTP copolymers. The PTP copolymers were synthesized as follows. ACVA, TMPM and PDP with a certain molar feed ratio were dissolved in a 0.75 M aqueous HCl solution. The solution was heated at ~ 70 °C for ~ 12 h under magnetic stirring after removing oxygen by three cycles of freeze-thaw process to prepare the P(TMPM-co-PDP) copolymers. Then, the certain amounts of $Na_2WO_4 \cdot 2H_2O$, EDTA, and

aqueous NaOH solution (10 wt%) were added to the as-prepared solution under stirring until the reagents were dissolved. Subsequently, the PTP-containing solution was obtained by the H_2O_2 oxidation for another 48 h at room temperature. Finally, the PTP solution was successively dialyzed in 1.0 M aqueous NaCl solution for 3 days and in water for 4 days.

Synthesis of StMV. MBI (1.2 g, 4.0 mmol) and 4-vinylbenzyl chloride (1.7 mL, 12.1 mmol) were added in 80 mL of acetonitrile solution under N_2 atmosphere, and then the mixture was stirred at 60 °C for 24 h. After the reaction was completed, the product was washed with acetonitrile several times using a vacuum filtration method until the filtered solution was clear and transparent.

Synthesis of the PVP copolymers. The PVP copolymers were synthesized as follows. Certain amounts of StMV, PDP, and ACVA were dissolved in 40 mL of water, and then the mixture was heated at 75 °C for 12 h after removing the oxygen from the aqueous solution. Finally, the PVP solution was successively dialyzed in 1.0 M aqueous NaCl solution for 3 days and in water for 4 days.

Preparation of the PPAT hydrogel. The details about the synthesis of 3-(adenine-9-yl)propyl acrylamide (AAm) and 3-(thymin-1-yl)propyl acrylamide (TAm) can be found elsewhere.[S1] The propylsulfonate dimethylammonium propylacrylamide (PDPA) was synthesized as follows. 1,3-Propanesulfonate (10 g, 81.9 mmol) and acetonitrile (5 g)

were added to an acetonitrile solution of DMAPAA (7.9 g, 50.5 mmol), and then the mixture was stirred at 25 °C for 24 h, followed by an additional 48 h of stirring in an ice bath. Finally, the product was dried under vacuum for 12 hours to obtain the PDPA.

The PPAT hydrogel was synthesized as follows. The alpha-ketoglutaric acid potassium salt (0.1 mmol %) was first dissolved in water (1 mL). Then, PDPA (0.33 g, 1.2 mmol), TAm (0.09 g, 0.4 mmol), and AAm (0.09 g, 0.4 mmol) were added to the above solution. Afterward, the obtained uniformly dispersed solution was exposed to the UV radiation at 365 nm for 8 h to get the PPAT hydrogel. The PPAT hydrogel was immersed in a 2.0 M aqueous LiCl solution for 24 h before the application as the separator.

Preparation of the electrode. The graphene suspension was prepared by dispersing graphene (1 g) in 200 mL of DMF, followed by successive sonication for 72 h and centrifugation at 3000 r/min for 30 min, to obtain the uniformly dispersed suspension. A 10 μL of N117 solution was added to 1 mL of graphene suspension, followed by a sonication for 2 min. Afterward, a 15 μL of the graphene/N117 solution was dropped on the glassy carbon (GC) electrode to prepare the graphene/GC electrode for the three-electrode measurements.

The graphene-based electrode for the planar configuration was prepared by the vacuum filtration of the graphene dispersion on the polyvinylidene fluoride microfiltration membrane, followed by a transfer of it onto the polyethylene terephthalate substrate, to obtain the graphene film. In the case of the full-cell

configuration, the PPAT hydrogel with a thickness of 1 mm was used as the separator and the copper wires were used as the current collectors.

Electrochemical tests. The cyclic voltammetry (CV), galvanostatic charge/discharge (GCD), and electrochemical impedance spectroscopy were measured at an electrochemical workstation (Bio-Logic VMP-300). For the three-electrode measurements, the graphene/GC electrode, Pt electrode, and Ag/AgCl electrode were respectively used as the working electrode, counter electrode, and reference electrode, where PTP or PVP dissolved in a 2.0 M LiCl solution was used as the electrolyte. For example, the concentration of TEMPO unit of PTP was fixed at 0.8 mM to determine the optimal feed ratio of PTP in terms of specific capacitance in a three-electrode system. For the half-cell configuration, the oversized graphene-based electrode was employed as the counter electrode. For the full-cell configuration, the 50 mM TEMPO unit of the P($TEMPO_{14}$-co-PDP_{86})/2.0 M LiCl and 2 mM StMV unit of the P($StMV_{13}$-co-PDP_{87})/2.0 M LiCl were employed as the electrolyte.

Other characterizations. The ^{1}H NMR spectra were recorded on a Bruker AV400 spectrometer. Weight average molar mass (M_w) of the copolymers were determined by a size exclusion chromatography (SEC) (Waters 1515) with 1.0 M $NaNO_3$ as the eluent and a flow rate of 1 mL min^{-1}. UV-Vis spectra were measured using the UNICO 2802 UV-Visible spectrophotometer.

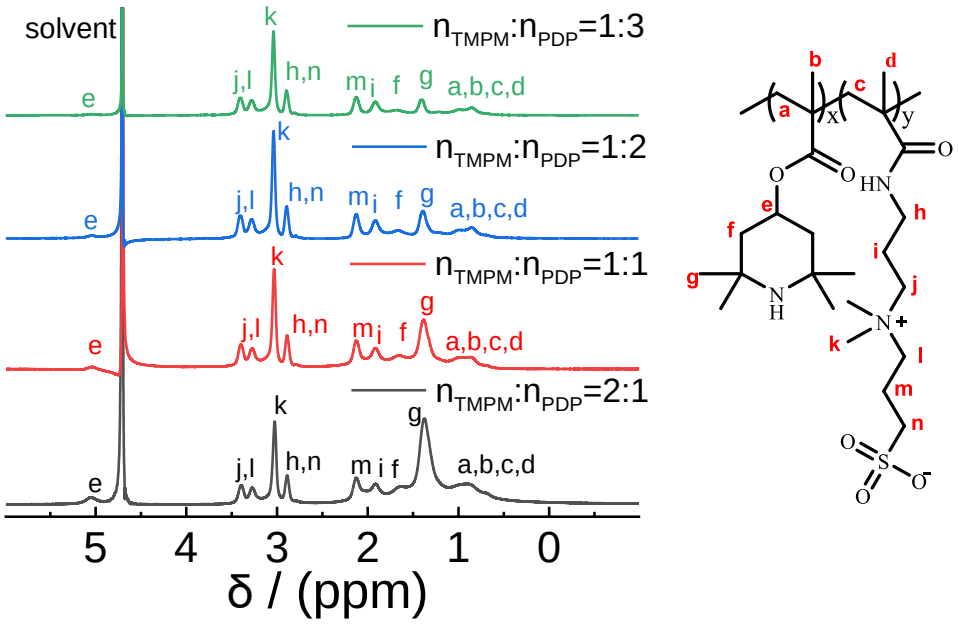

Fig. S1. ^{1}H NMR spectra of the P(TMPM-co-PDP) copolymers with different feed ratios.

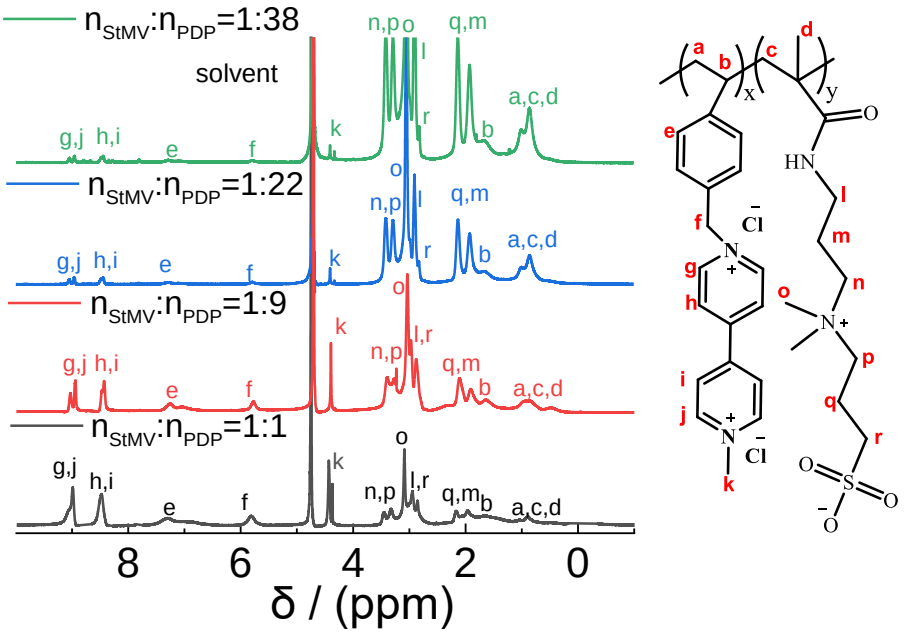

Fig. S2. ^{1}H NMR spectra of the P(StMV-co-PDP) copolymers with different feed ratios.

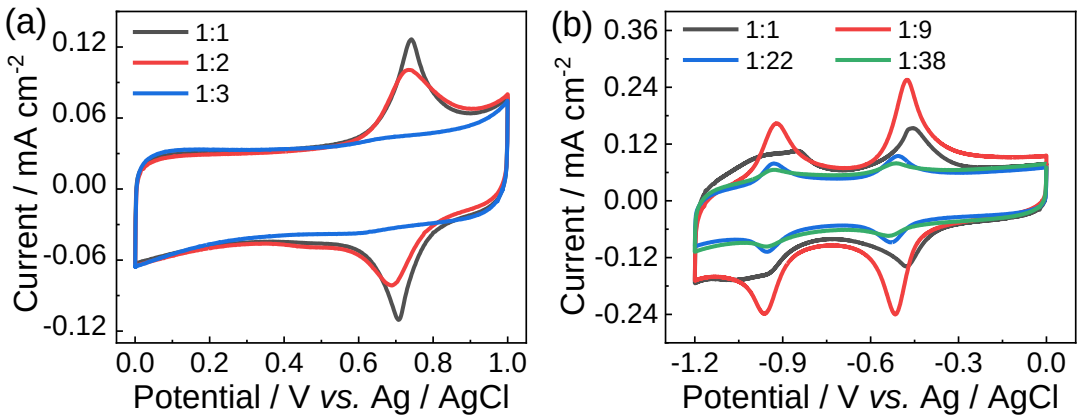

Fig. S3. CV curves for the polymeric redox couples at a scan rate of 100 mV s^{-1} in the three-electrode measurements. (a) PTP as a function of the feed ratio between TMPM and PDP, and (b) PVP as a function of the feed ratio between StMV and PDP.

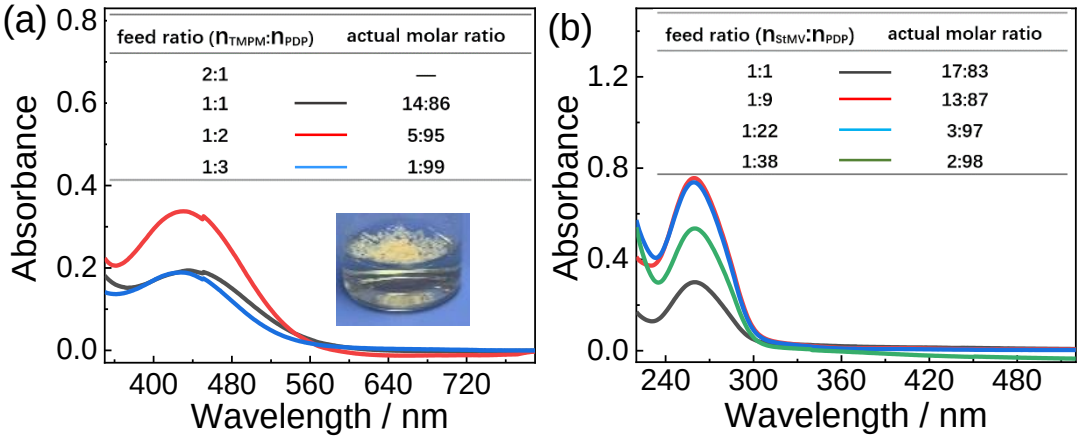

Fig. S4. The UV-Vis spectra of PTP and PVP with different feed ratios, where the actual molar ratios of these polymeric redox couples can be determined. (a) PTP, the inset shows that PTP with the feed ratio of 2:1 between TMPM and PDP is insoluble in water. (b) PVP.

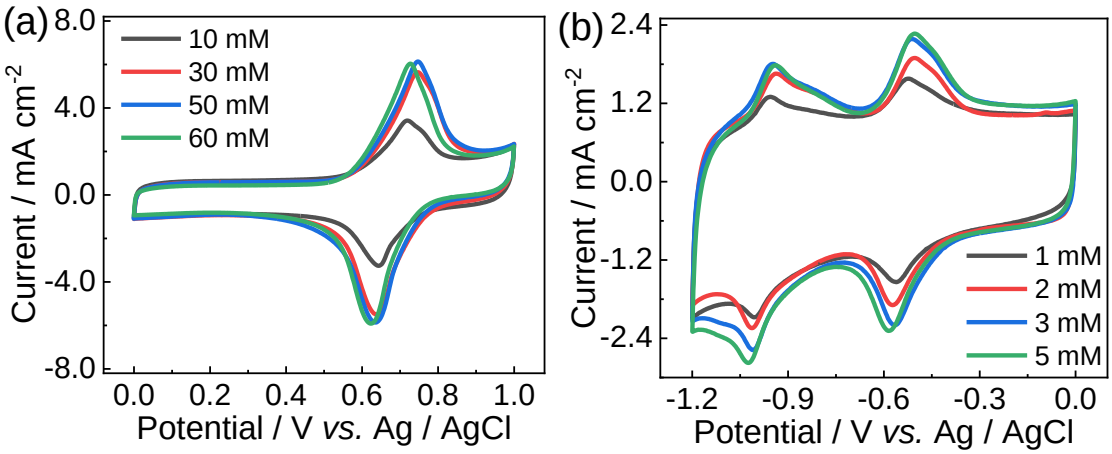

Fig. S5. (a) The CV curves of P($TEMPO_{14}$-co-PDP_{86}) with different concentrations of TEMPO unit in a half-cell configuration at a scan rate of 100 mV s^{-1}. (b) The CV curves of P($StMV_{13}$-co-PDP_{87}) with different concentrations of StMV unit in a half-cell configuration at a scan rate of 100 mV s^{-1}.

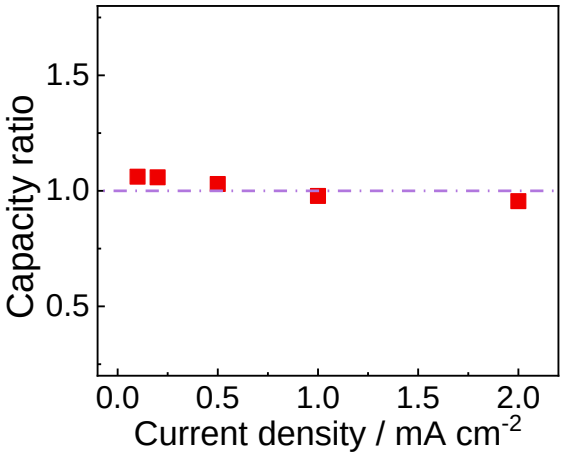

Fig. S6. The capacity ratio between negative and positive electrodes, where the molar concentration of StMV unit in P($StMV_{13}$-co-PDP_{87}) is fixed at 2 mM and the molar concentration of TEMPO unit in P($TEMPO_{14}$-co-PDP_{86}) is fixed at 50 mM.

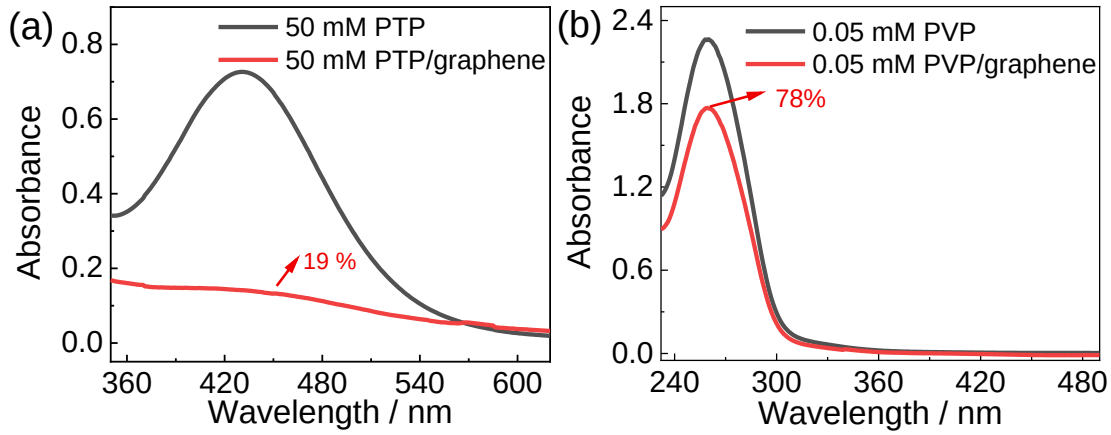

Fig. S7. UV-Vis spectra of the polymeric redox couples in the absence or presence of 0.5 mg mL^{-1} graphene. (a) P($TEMPO_{14}$-co-PDP_{86}), and (b) P($StMV_{13}$-co-PDP_{87}). The percentage number in panels (a) and (b) indicates the percentage of the corresponding copolymer remained in the solution after the adsorption on the graphene surface for 24 h.

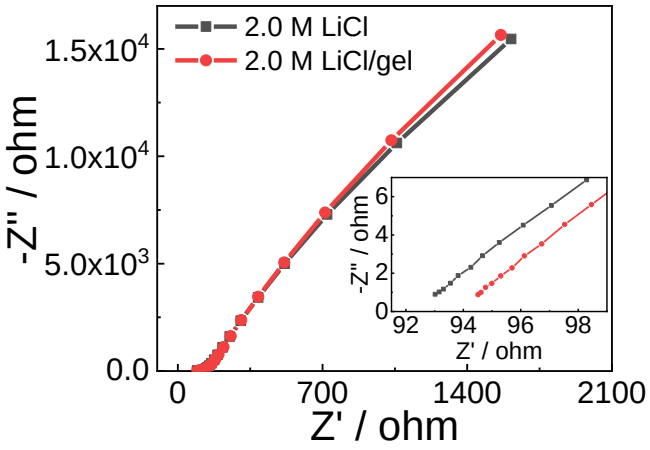

Fig. S8. The electrochemical impedance spectra of the supercapacitors employing a 2.0 M LiCl solution as the electrolyte in the absence or presence of 1 mm of PPAT gel separator.

In Fig. S8, the bulk resistances of the supercapacitors employing a 2.0 M LiCl solution as the electrolyte are comparable in the absence (93.0 Ω) or presence (94.5 Ω) of 1 mm of PPAT gel separator.

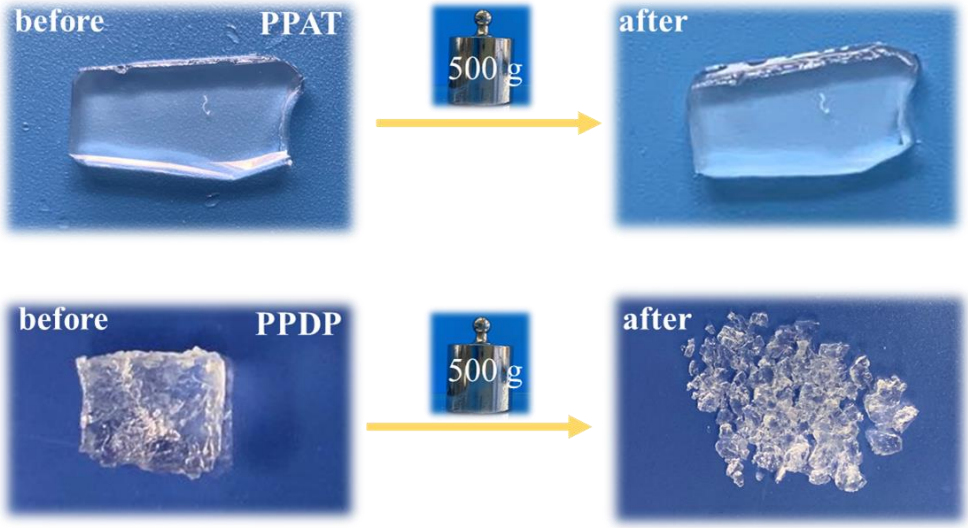

Fig. S9. The images of PPAT and PPDP hydrogels after immersing in a 2.0 M LiCl solution for 24 h being compressed by a 500 g weight. (a) PPAT, and (b) PPDP. Here, the PPAT hydrogel is tougher than the covalent-crosslinked PPDP hydrogel.

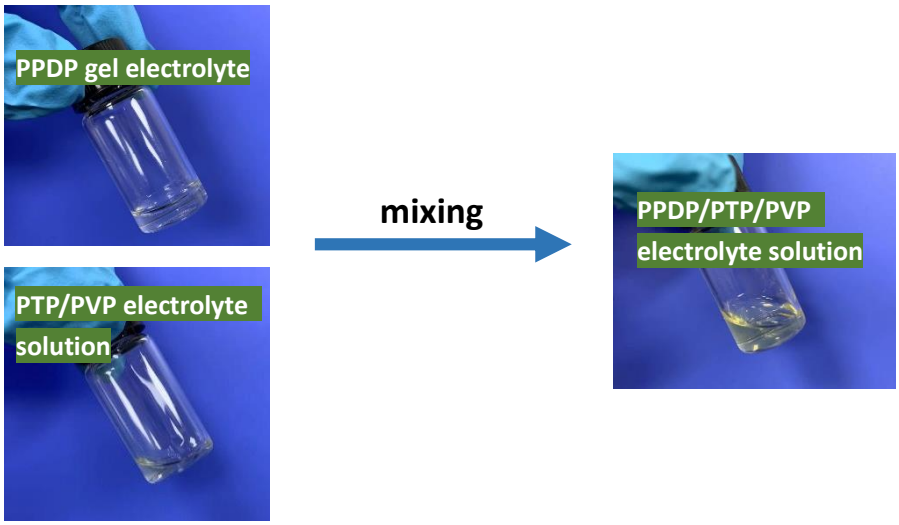

Fig. S10. The images showing the dissolution of PPDP gel electrolyte in the polymer electrolyte solution. Here, the PPDP gel electrolyte is prepared by the solvent evaporation method.

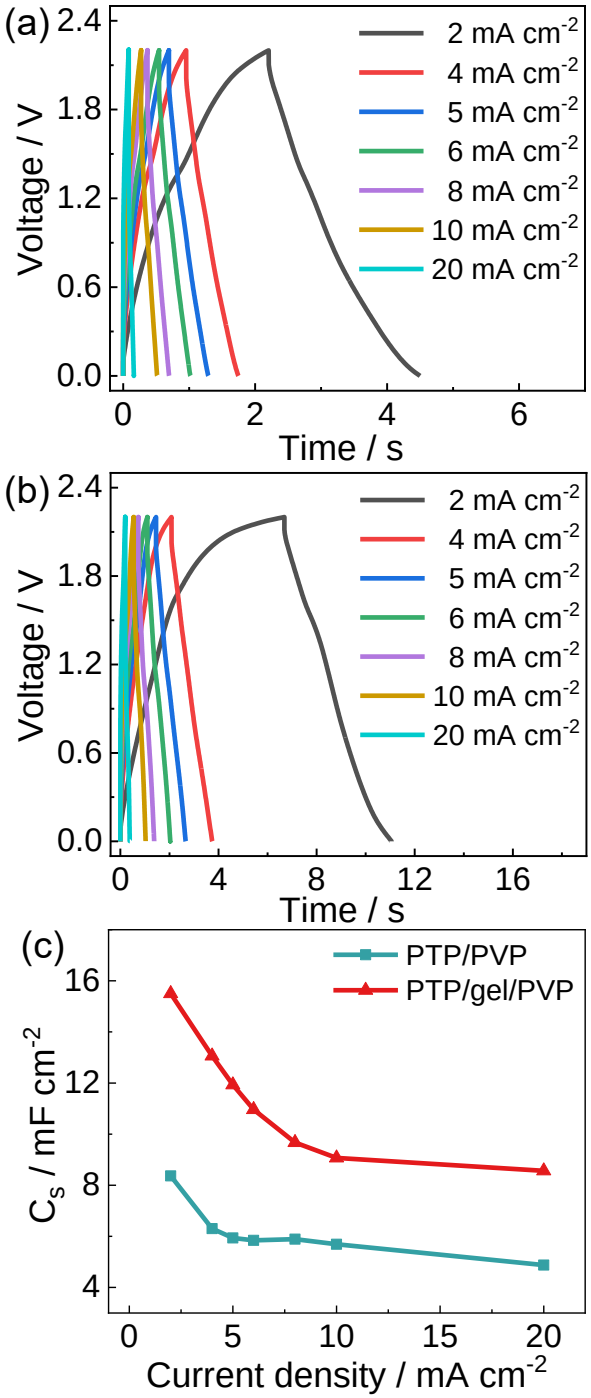

Fig. S11. (a) The GCD curves of the PTP/PVP-based supercapacitor at different current densities. (b) The GCD curves of the PTP/gel/PVP-based supercapacitor at different current densities. (c) C_s of the PTP/PVP- and PTP/gel/PVP-based supercapacitors as a function of current density.

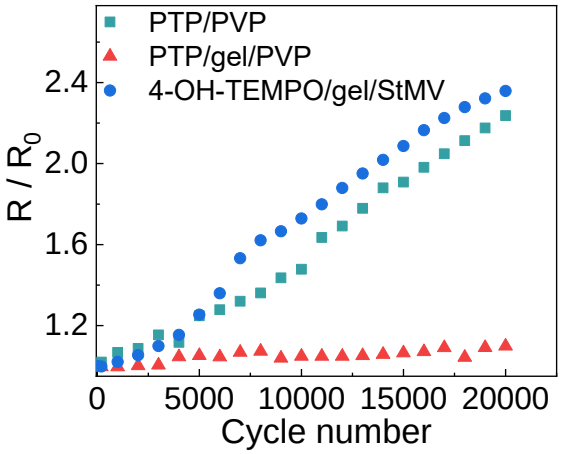

Fig. S12. The change in relative resistance (R/R_0) as a function of cycle number during the tests of cycling performance at a current density of 5.0 mA cm^{-2} in the GCD measurements for the PTP/PVP-, PTP/gel/PVP-, and 4-OH-TEMPO/gel/StMV-based supercapacitors.

According to the previous studies,[S2,S3] the decrease in capacitance retention for both the PTP/PVP- and 4-OH-TEMPO/gel/StMV-based supercapacitors with increasing cycle number could be correlated with the increase in resistance.

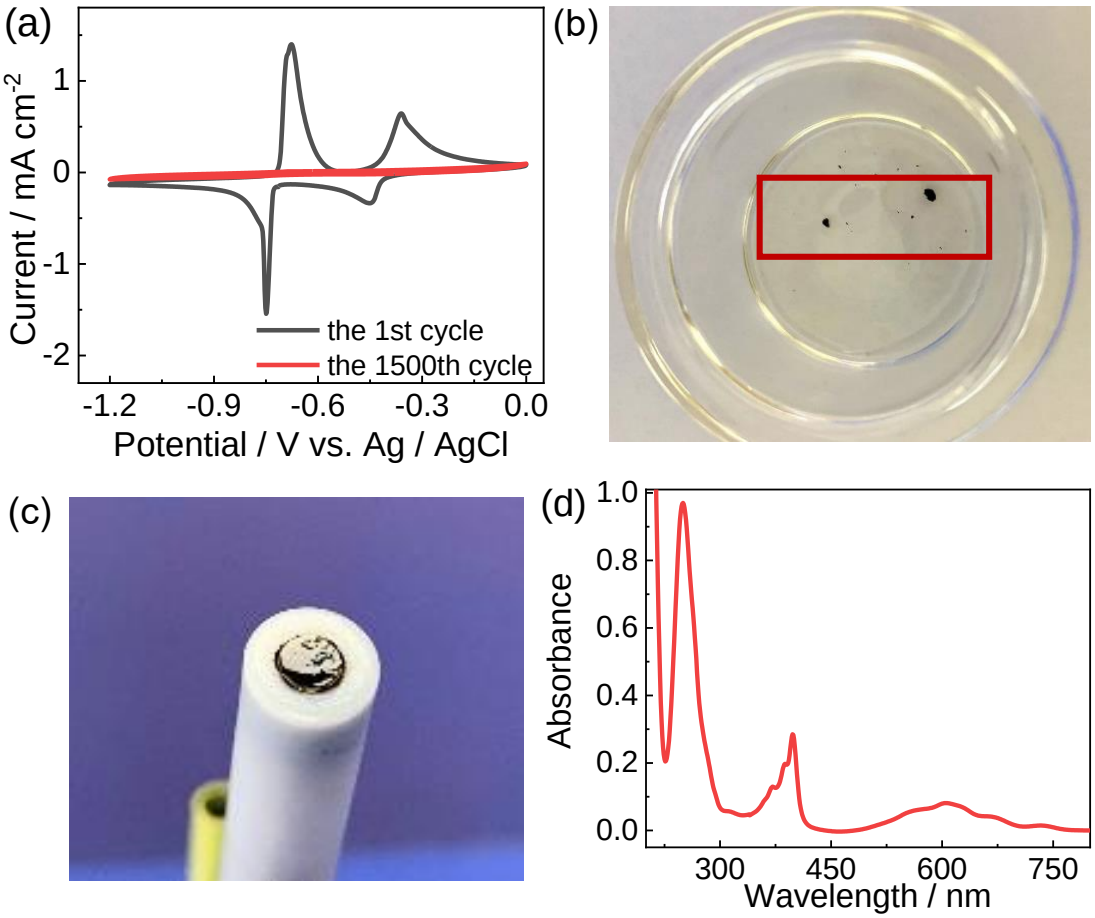

Fig. S13. (a) The CV curves of an aqueous electrolyte solution composed of 2 mM StMV and 2.0 M LiCl in the three-electrode system at the 1st and 1500th cycles. (b) The image of the $StMV^{+\bullet}$ precipitant in the aqueous electrolyte solution. (c) The $StMV^{+\bullet}$ precipitant on the surface of the GC electrode. (d) The UV-Vis spectrum of the $StMV^{+\bullet}$ precipitant dissolved in acetonitrile.

In Fig. S13a, almost no redox peaks can be observed in the CV curve for the aqueous electrolyte solution composed of 2 mM StMV and 2.0 M LiCl after 1500 cycles of tests in the three-electrode system. This is due to the precipitation of the $StMV^{+\bullet}$ in the aqueous electrolyte solution and the deposition of the $StMV^{+\bullet}$ precipitant on the surface of GC electrode, as confirmed by the results shown in Fig. S13b and Fig. S13c. The result in Fig. S13d confirms that the precipitant in Fig. S13b and Fig. S13c is $StMV^{+\bullet}$.[S4,S5]

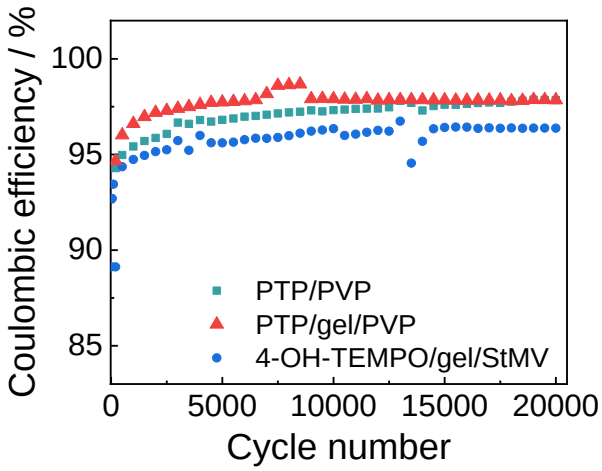

Fig. S14. The Coulombic efficiency as a function of cycle number obtained at a current density of 5.0 mA cm^{-2} in the GCD measurements for the PTP/PVP-, PTP/gel/PVP-, and 4-OH-TEMPO/gel/StMV-based supercapacitors.

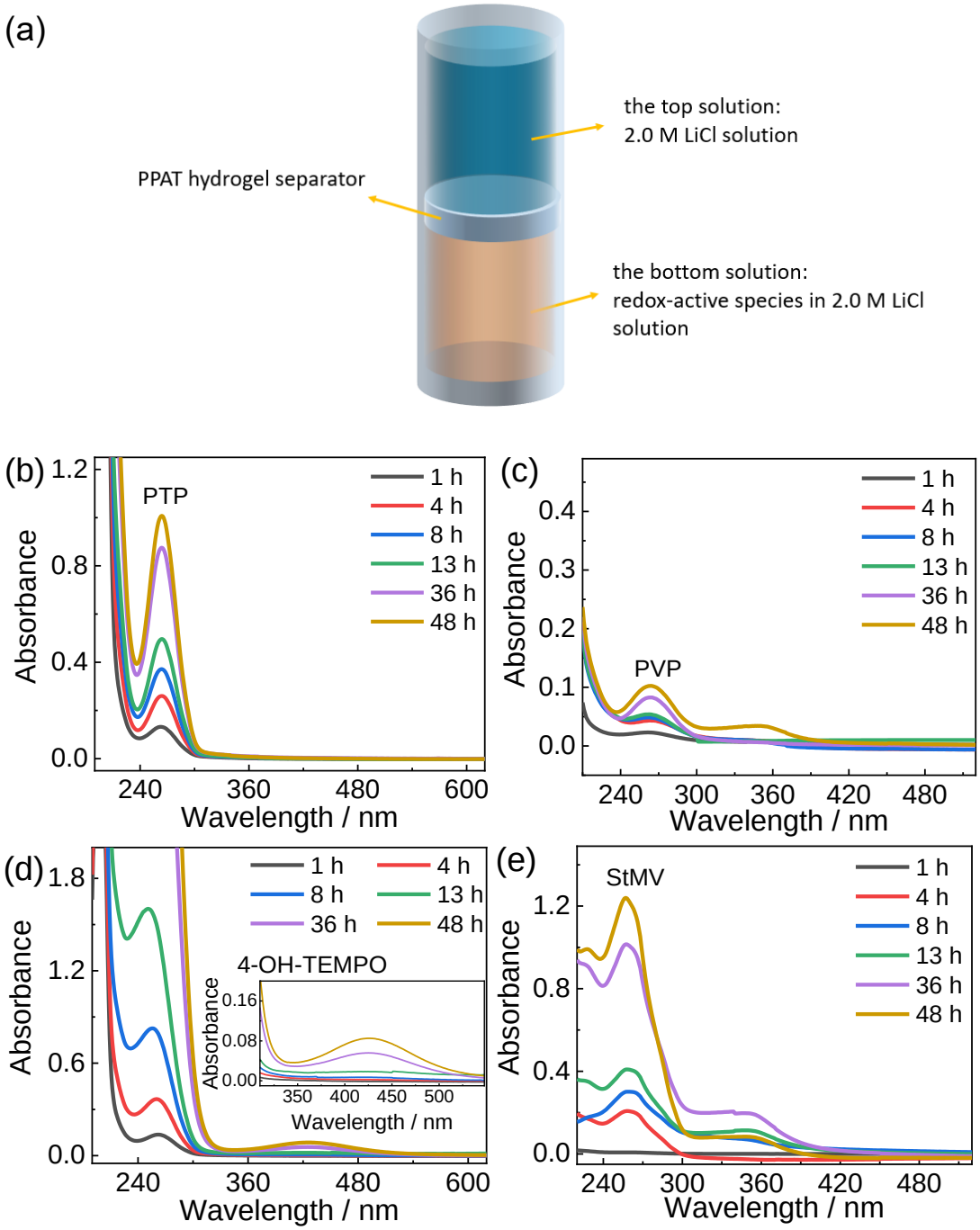

Fig. S15. (a) Schematic illustration of the measurements of the diffusion of the redox-active species through the PPAT hydrogel separator. (b) Time dependence of UV-Vis spectra of PTP in the top solution, where the concentration of the redox-active unit of PTP in the bottom solution is fixed at 50 mM. (c) Time dependence of UV-Vis spectra of PVP in the top solution, where the concentration of the redox-active unit of PVP in the bottom solution is fixed at 2 mM. (d) Time dependence of UV-Vis spectra of 4-OH-TEMPO in the top solution, where the concentration of 4-OH-TEMPO in the bottom solution is fixed at 50 mM. (e) Time dependence of UV-Vis spectra of StMV in the top solution, where the concentration of StMV in the bottom solution is fixed at 2 mM.

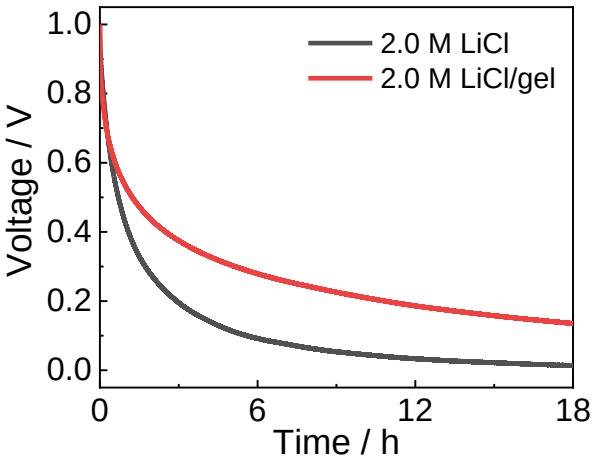

Fig. S16. Time dependence of the decay of voltage of the supercapacitors employing a 2.0 M LiCl solution as the electrolyte in the absence or presence of the PPAT hydrogel separator.

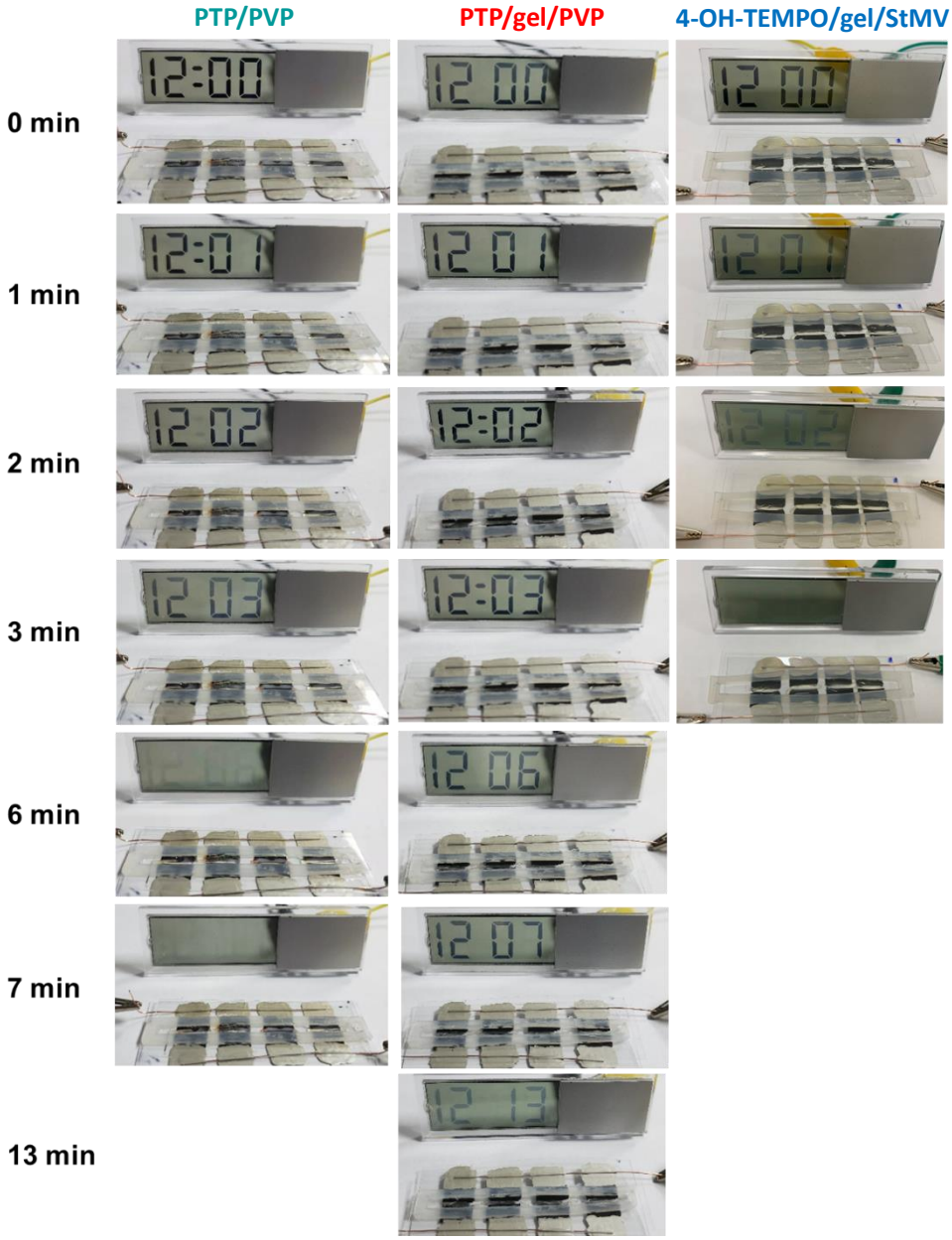

Fig. S17. The images of the liquid crystal display electronic watches powered by the PTP/PVP-, PTP/gel/PVP-, and 4-OH-TEMPO/gel/StMV-based supercapacitors.

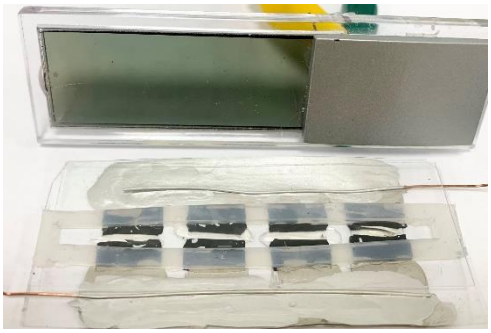

Fig. S18. The image of the liquid crystal display electronic watch powered by the 2.0 M LiCl-based supercapacitor at the initial time.

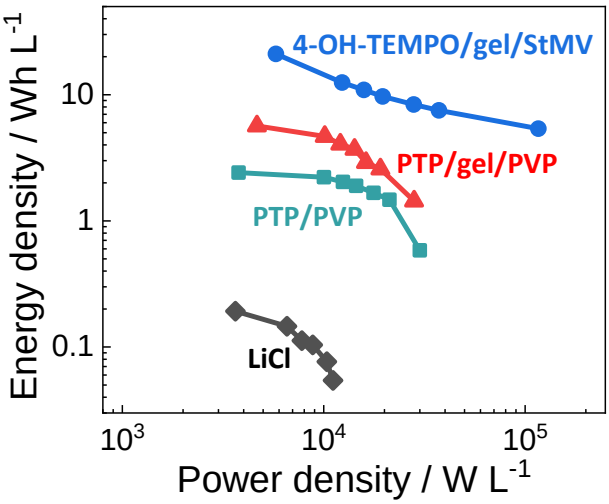

Fig. S19. The Ragone plots of the 2.0 M LiCl-, PTP/PVP-, PTP/gel/PVP-, and 4-OH-TEMPO/gel/StMV-based supercapacitors.

Table S1. Molecular parameters of the PTP copolymers determined by SEC.

feed ratio (n_{TMPM}:n_{PDP})	M_w / (g mol^{-1})
1:1	~ 7.0 x 10^4
1:2	~ 1.0 x 10^5
1:3	~ 1.1 x 10^5

Table S2. Molecular parameters of the PVP copolymers determined by SEC.

feed ratio (n_{StMV}:n_{PDP})	M_w / (g mol^{-1})
1:1	~ 6.0×10^3
1:9	~ 2.9×10^5
1:22	~ 4.9×10^5
1:38	~ 5.7×10^5

References

S1. Z. Hua, B. Pitto, Anaïs, Y. Kang, N. Kirby, T. R. Wilks and R. K. O'Reilly, *Polym. Chem.*, 2016, **7**, 4254-4262.

S2. P. Ratajczak, K. Jurewicz, P. Skowron, Q. Abbas and F. Béguin, *Electrochim. Acta.*, 2014, **130**, 344-350.

S3. P. Ratajczak, K. Jurewicz and F. Béguin, *J. Appl. Electrochem.*, 2014, **44**, 475-480.

S4. H. Chen, V. Brasiliense, J. Mo, L. Zhang, Y. Jiao, Z. Chen, L. O. Jones, G. He, Q. H. Guo, X. Y. Chen, B. Song, G. C. Schatz and J. F. Stoddart, *J. Am. Chem. Soc.*, 2021, **143**, 2886-2895.

S5. H. Qu, M. Harada and T. Okada, *ChemElectroChem*, 2017, **4**, 35-38.